Research Paper

The toxicity of lead to *Desulfovibrio desulfuricans* G20 in the presence of goethite and quartz

Rajesh K. Sani[*,1], Gurdeep Rastogi[*,#,1], James G. Moberly[2], Alice Dohnalkova[3], Timothy R. Ginn[4], Nicolas Spycher[5], Rajesh V. Shende[1], Brent M. Peyton[2]

[1] Department of Chemical and Biological Engineering, South Dakota School of Mines and Technology, Rapid City, SD, USA
[2] Department of Chemical and Biological Engineering, Montana State University, Bozeman, MT, USA
[3] Environmental Molecular Sciences Laboratory, Pacific Northwest National Laboratory, Richland, WA, USA
[4] Department of Civil and Environmental Engineering, University of California, Davis, CA, USA
[5] Geochemistry Department, Earth Science Division, Lawrence Berkley National Laboratory, Berkley, CA, USA

An aqueous mixture of goethite, quartz, and lead chloride ($PbCl_2$) was treated with the sulfate-reducing bacterium, *Desulfovibrio desulfuricans* G20 (*D. desulfuricans* G20), in a medium specifically designed to assess metal toxicity. In the presence of 26 μM of soluble Pb, together with the goethite and quartz, *D. desulfuricans* G20 grew after a lag time of 5 days compared to 2 days in Pb-, goethite-, and quartz-free treatments. In the absence of goethite and quartz, however, with 26 μM soluble Pb, no measurable growth was observed. Results showed that *D. desulfuricans* G20 first removed Pb from solutions then growth began resulting in black precipitates of Pb and iron sulfides. Transmission electron microscopic analyses of thin sections of *D. desulfuricans* G20 treated with 10 μM $PbCl_2$ in goethite- and quartz-free treatment showed the presence of a dense deposit of lead sulfide precipitates both in the periplasm and cytoplasm. However, thin sections of *D. desulfuricans* G20 treated with goethite, quartz, and $PbCl_2$ (26 μM soluble Pb) showed the presence of a dense deposit of iron sulfide precipitates both in the periplasm and cytoplasm. Energy-dispersive X-ray spectroscopy, selected area electron diffraction patterns, or X-ray diffraction analyses confirmed the structure of precipitated Pb inside the cell as galena (PbS) in goethite- and quartz-free treatments, and iron sulfides in treatments with goethite, quartz, and $PbCl_2$. Overall results suggest that even at the same soluble Pb concentration (26 μM), in the presence of goethite and quartz, apparent Pb toxicity to *D. desulfuricans* G20 decreased significantly. Further, accumulation of lead/iron sulfides inside *D. desulfuricans* G20 cells depended on the presence of goethite and quartz.

Keywords: Heavy metals / Iron minerals / Sulfate-reducing bacteria / Pb-toxicity

Received: July 25, 2009; accepted: October 01, 2009

DOI 10.1002/jobm.200900239

Introduction

Lead and its inorganic compounds are (i) classified as carcinogens, (ii) are toxic to most biota at elevated exposures, and (iii) have no known biological functions [29]. The most common sources of Pb contaminations are battery plates, Pb-based paints, glazes on dishware, and Pb-pipes containing water for long periods. Additionally, Pb is one of the most common heavy-metal contaminant found in United States Department of Energy (U.S. DOE) sites, where solid and liquid wastes were discharged to the ground [14, 20]. These metals and metal chelates threaten down-gradient water resources; thus, they are of particular environmental concern.

*The first two authors made equal contributions to this work.
#Present address: Department of Plant Pathology, University of California, Davis, CA, 95616, USA.
Correspondence: Rajesh K. Sani, Department of Chemical and Biological Engineering, South Dakota School of Mines and Technology, Rapid City, SD 57701, USA
E-mail: Rajesh.Sani@sdsmt.edu
Phone: 605-394-1240
Fax: 605-394-1232

Heavy-metal contaminated environments pose difficult challenges in remediation; however, microbiological processes can be used for *in situ* immobilization of many metals and radionuclides [13]. For example, sulfate-reducing activity can produce sulfide, which can decrease metal mobility and bioavailability by forming insoluble metal-sulfide precipitates [15]. Sulfate-reducing bacteria (SRB) have been observed in many contaminated subsurface sites and stimulating them has potential remediation value [1]. SRB are known to enzymatically reduce Cr(VI), Tc(VII), and U(VI), to form insoluble mineral phases, and have also been shown to reduce Fe(III) and Mn(IV) [15]. SRB can catalyze a variety of heavy metal transformations, however, it has been demonstrated that heavy metals at toxic levels can inhibit or prevent SRB growth [4, 10, 16, 19, 24, 25, 31]. An increase in soluble metal concentrations can decrease sulfate reduction rates, causing a decrease in metal sulfide production. Effective manipulation of an indigenous sulfate-reducing bacterial community to stimulate *in situ* bioremediation activity requires knowledge of the toxic effects of various heavy metals on SRB in the presence of soil minerals. Existing literature shows the toxicity of Cd, Cu, Cr, Ni, Mn, U, and Zn to SRB are well documented, however, investigations of Pb toxicity to SRB is scarce [22, 27]. White et al. [33] showed that in metal (Cd, Co, Cr, Cu, Mn, Ni, Pb, and Zn)-contaminated soils, SRB remained metabolically active. The surfaces of soil minerals have strong capabilities to adsorb metal ions and therefore reduce aqueous concentrations to a non-toxic levels, and decreasing overall metal bioavailability [3]. Several studies were conducted which show the effects of toxic heavy metals on pure or mixed SRB in the absence of soil minerals using microbial growth media containing metal complexants/precipitants which reduce the effective soluble metal concentration available to targeted SRB [10, 19, 31]. To develop effective *in situ* or *ex situ* bioremediation technologies, there must be a better understanding of the effects of heavy metals on SRB in the presence of soil minerals.

Our previous published results [22, 24, 27] showed that using a metal toxicity medium (MTM), which was specifically designed to eliminate the formation of metal precipitates and minimize metal complexation, $PbCl_2$ was much more toxic to *D. desulfuricans* G20 than previously thought. These studies provided fundamental relevance to SRB found in natural systems that contain $PbCl_2$, and also to efforts to use SRB to remediate $PbCl_2$ contamination. However, use of MTM and a pure culture of *D. desulfuricans* G20 may overestimate $PbCl_2$ toxicity in natural environments such as DOE sites where chemical complexants including iron minerals are presents. These iron minerals can reduce the metal bioavailability to SRB and hence the toxicity. Therefore the present study carefully evaluated the effects of $PbCl_2$ to *D. desulfuricans* G20 in the presence of presence of goethite and quartz as model redox-sensitive and -insensitive aquifer minerals [24], respectively. We hypothesized that in the presence of natural metal specific ligands, the toxicity of Pb(II) to *D. desulfuricans* G20 will significantly be decreased. Supplementation of MTM with these natural ligands will help better understand the interactive effects of aqueous system components and bioavailability of toxic heavy metals to SRB and also to efforts to use SRB to remediate Pb(II) contamination. Therefore to test this hypothesis in the present study, MTM, soil minerals, and a pure culture of *D. desulfuricans* G20 were used to develop a more fundamental understanding of SRB exposed to Pb in a defined system mimicking natural conditions. The present study evaluated Pb inhibition on a model SRB, *D. desulfuricans* G20 in the presence of goethite and quartz as model redox-sensitive and -insensitive aquifer minerals [6], respectively. The Pb/goethite system was chosen because Pb is a major pollutant in soils and U.S. DOE sites nationwide, and because goethite is a common soil constituent capable of adsorbing large quantities of metals [3, 6].

Materials and methods

Synthesis and characterization of goethite and quartz

The Fe(III)-oxyhydroxide, goethite (α-FeOOH) was synthesized as described previously [28]. A Coulter SA 3100 BET analyzer (using N_2 sorption) was used to determine the specific surface area of the goethite and quartz grains (α-SiO_2, 212–300 μm), which were found to be 52 and 0.02 m^2/g, respectively. The size and shape of the goethite crystals were examined by means of electron microscopy using the methods described earlier [11]. Electron microscopic observation showed that synthetic goethite crystals were of uniform shape and size, and crystals were similar to those found in natural environments [28]. Goethite crystals were euhedral, needle-like in shape, about 200 nm (±20) in length and 25 nm (±5) in diameter (images are not shown). A previous study by Fredrickson *et al.* [7] showed potential phase modifications in goethite due to sterilization by autoclaving; therefore in this study, the goethite was not autoclaved. However, prior to use, the goethite and quartz minerals were heat-treated in pre-sterilized culture tubes in an oven at 80 °C for 16 h. No measurable

change in specific surface area occurred as a result of this treatment [23, 26].

Medium and cultivation conditions

D. desulfuricans G20 was a generous gift of Dr. Judy Wall, University of Missouri-Columbia USA. *D. desulfuricans* G20 contains the green fluorescent protein (GFP) reporter gene construct. The GFP was unused in the present study, but to maintain the GFP construct, 20 μg/ml chloramphenicol was added which also conferred chloramphenicol resistance. In addition, previous metal (Pb, Cu, and U) toxicity studies in *D. desulfuricans* G20 [22, 24, 25, 27], and other study that involved direct non-destructive microscopic observations of *D. desulfuricans* G20 on mineral surfaces [17] contained chloramphenicol in all treatments. Therefore to compare (and to be consistent) with these earlier studies, chloramphenicol was added to MTM in all treatments prior to inoculation. Serum bottle preparation and cultivation conditions were the same as described previously [27]. Water used in all experiments was supplied from a Barnstead Nanopure water purification system with a resistivity of 17.6 MΩ · cm. All glassware was washed with 2 N HNO_3 and rinsed with nanopure water.

Lead adsorption and immobilization experiments

The adsorption of Pb onto minerals (goethite and quartz) was studied in batch experiments in MTM containing lactate and sulfate at 30 and 10 mM, respectively. The medium pH was adjusted to 7.2 using 6 N HCl. Controls included Pb-, *D. desulfuricans* G20-, mineral-, sulfate-, and lactate-free MTM treatments (Table 1). Volumes of 120-ml of medium in 150-ml serum bottles were autoclaved separately. A filtered (0.2 μm, Gelman acrodisc syringe filter) stock solution of $PbCl_2$ (4.8 mM) was aseptically added to the serum bottles to achieve a final Pb concentration of 70 μM. After thorough mixing, samples were withdrawn aseptically to measure initial concentrations of soluble Pb, lactate, and sulfate. Heat-treated goethite and quartz at a ratio of 1:19 (80 and 1520 mg, respectively) were added to serum bottles containing Pb and MTM. Typical redox-sensitive mineral concentrations (e.g., iron minerals) found in soils range from 0.5 to 6% (w/w) [18] therefore 5% (w/w) goethite in goethite-quartz mixture was used in present study. Serum bottles were capped with butyl-rubber septa, crimped with aluminum seals, purged, and pressurized with ultra-pure N_2 (g) at 68.9 kPa (10 psi) above atmospheric pressure. The bottles were incubated at 25 °C in a horizontal position on an orbital shaker at 125 rpm. Under abiotic conditions, samples were collected over a 9-day period to monitor the establishment of Pb equilibrium between the soluble and solid phases.

Four-day-grown *D. desulfuricans* G20 cultures were centrifuged in the presence of ultra-pure N_2(g) at 10,000 × *g* for 15 min. The supernatant was discarded and the cell pellets were suspended in anaerobic 0.89% NaCl solution. This process was repeated twice, and washed cells were used as inoculum. After abiotic equilibration of Pb for 9 d (after which no further significant decrease in soluble Pb concentration was observed, Fig. 1), washed cells of *D. desulfuricans* G20 were anaerobically injected into serum bottles to achieve 3 mg/l initial total cell protein. After inoculation, serum bottles were incubated at 25 °C in an orbital shaker at 125 rpm. Periodically, 3-ml samples were analyzed for total cell protein, soluble Pb, and sulfide. At the end of the experiments, concentrations of lactate, sulfate, and acetate were measured.

A previous study of Pb toxicity to *D. desulfuricans* G20 showed a minimum inhibitory concentration (MIC) of Pb at 15 μM [27]. However, the fate of Pb and structure of lead sulfide precipitates formed during the growth of *D. desulfuricans* G20 were not examined. Therefore, treatment I was started on day 9 in which Pb was added at a final concentration of 10 μM. *D. desulfuricans* G20 cells, collected from this treatment were studied using TEM, EDS, and XRD to observe Pb localization and the elemental composition and structure of precipitated materials.

Estimation of Pb(II), organic and inorganic anions, and cell protein concentration

Samples for soluble Pb concentrations were filtered (0.2 μm), diluted in 3% HNO_3, and measured on an Agilent 4500 inductively coupled plasma mass spectrometer (ICP-MS) [27]. Soluble sulfide concentrations were determined spectrophotometrically using the methylene blue method (Hach, Loveland, CO, USA) [27]. Samples for lactate, sulfate, and acetate analysis were filtered (0.2 μm) and concentrations were determined using a Dionex DX-500 Ion Chromatograph (IonPac AS11-HC4-mm column, conductivity detection) (Dionex, Sunnyvale, CA, USA) with an estimated error of ±5% [27]. Total cell protein was determined using a quantitative colorimetric Coomassie assay as described previously [22]. Each set of experiments was carried out in duplicate and repeated three times. In each experiment, duplicate treatment profiles were very similar in total cell protein, Pb, and sulfide concentrations; however, the length of the lag time was somewhat variable. Similar variability in lag times for different experiments using *D. desulfuricans* and *Shewanella oneidensis* MR-1 has been observed in the presence of metals including Cr, Cu, Ni, Pb, and Zn [19, 27, 32]. One-way analysis of variance (ANOVA) was used to determine if there were

statistically significant differences in *D. desulfuricans* G20 lag times among controls, and treatments containing Pb, with and without minerals. The threshold level of statistical significance for this study was $\alpha = 0.05$.

Transmission electron microscopy (TEM), energy-dispersive X-ray spectroscopy (EDS), and selected area electron diffraction (SAED) analyses

For TEM, due to the oxygen-sensitive nature of the samples, the whole embedding procedure, as well as thin sectioning, was conducted in an anaerobic glove box ($Ar:H_2$, 95:5; Coy Laboratory Products, Grass Lake, MI, USA). Stationary phase *D. desulfuricans* G20 cells collected from MTM containing (i) Pb, minerals, and *D. desulfuricans* G20 (test, treatment E), (ii) minerals and *D. desulfuricans* G20 (Pb-free controls, treatment H), and (iii) Pb and *D. desulfuricans* G20 (mineral-free control with 10 μM Pb, treatment I) were fixed in 2.5% glutaraldehyde, washed in anoxic deionized water followed by a gradual dehydration in ethanol series, and infiltration in LR White embedding resin (Electron Microscopy Sciences, Hatfield, PA, USA). Blocks were cured at 60 °C for 24 h, and sectioned to 70 nm thickness on a microtome (Leica Ultracut, UCT, Bannockburn, IL, USA). The sections were mounted on 200-mesh copper grids coated with formvar-support film sputtered with carbon, and examined using JEOL 2010 high-resolution transmission electron microscope (JEOL, Peabody, MA, USA) equipped with a LaB_6 filament operating at 200 kV with a resolution of 0.19 nm. Elemental analysis was performed using an Oxford energy dispersive spectroscopy system equipped with a SiLi detector coupled to the transmission-electron microscope and spectra were analyzed with ISIS software (Oxford Instruments, Abingdon, Oxfordshire, UK). Images were digitally collected and analyzed using the Digital Micrograph software (Gatan Inc., Pleasanton, CA, USA). The *d*-spacings obtained from the selected-area electron diffraction ring patterns were evaluated by Desktop Microscopist software (Lacuna, Beaverton, OR, USA).

X-ray diffraction (XRD) analyses

For XRD analyses, samples (treatments: B – MTM, Pb, and minerals; E – MTM, Pb, minerals, and *D. desulfuricans* G20; H – MTM, minerals, and *D. desulfuricans* G20; and I – MTM, Pb, and *D. desulfuricans* G20) were recovered at the end of experiments and centrifuged ($10{,}000 \times g$ for 10 min) under anaerobic conditions. After decanting the supernatant, the solid samples were dried at 25 °C temperature in a glove box (Model 1025, Forma Scientific Inc., Marietta, OH, USA) under an $N_2:CO_2:H_2$ (90:5:5) atmosphere. Dried samples were ground to a fine powder in a corundum mortar and pestle, and mixed in ethanol. The sample droplets were deposited uniformly on a low background quartz slide and were scanned on the Rigaku Geigerflex RU200b series diffractometer (Woodlands, TX, USA). The radiation source was CuK_α with a tube voltage and current of 50 kV and 160 mA, respectively. All samples were scanned from a 2θ of 3 to 70° with the step size of 0.02° and peaks obtained were identified using Jade (version 5.0) X-ray diffraction software.

Results and discussion

Pb adsorption under abiotic conditions

The first nine days of treatments; A, B, C, D, and E, contained abiotic equilibration of Pb with medium components and/or the minerals added to MTM. Soluble Pb concentration profiles during this equilibration period are shown in Fig. 1. It can be seen from Fig. 1 that three distinct Pb concentration profiles were observed. In treatment A (mineral and *D. desulfuricans* G20-free control), the soluble Pb concentration decreased from 70 to 58 μM during the first thirteen days (likely due to sorption to the glass of the serum bottles and reaction with medium components, and then remained almost constant through the end of the experiment (28 days). However, in treatment B (*D. desulfuricans* G20-free control), soluble Pb concentrations decreased to 29 μM in 9 d, and after that it decreased only slightly (to 26 μM) through the end of experiment (28 d) (Fig. 1). Thus most of the abiotic equilibration of Pb was completed in 9 days. The difference in soluble Pb concentrations between the abiotic treatments A and B is the result of adsorption or possibly, precipitation onto mineral surfaces [5]. Fig. 1 also shows that most adsorption of Pb (about 34 μM) onto goethite was observed within first 3 days of incubation followed by about 8 μM Pb sorption in next 6 days of incubation. From a kinetic perspective, the soluble Pb concentration decreased most sharply in the first day incubation, and most adsorption between the solution and solid phase was complete within 9 d. Previous studies have shown that adsorption of Pb onto goethite was complete within 4 h under very well defined conditions of Pb speciation and ionic strength (without microbial growth medium components) [6]. In the present study, however, the slower equilibration of Pb between the solution and solid phase may have resulted from organic and inorganic components present in MTM, which are necessary for microbial growth.

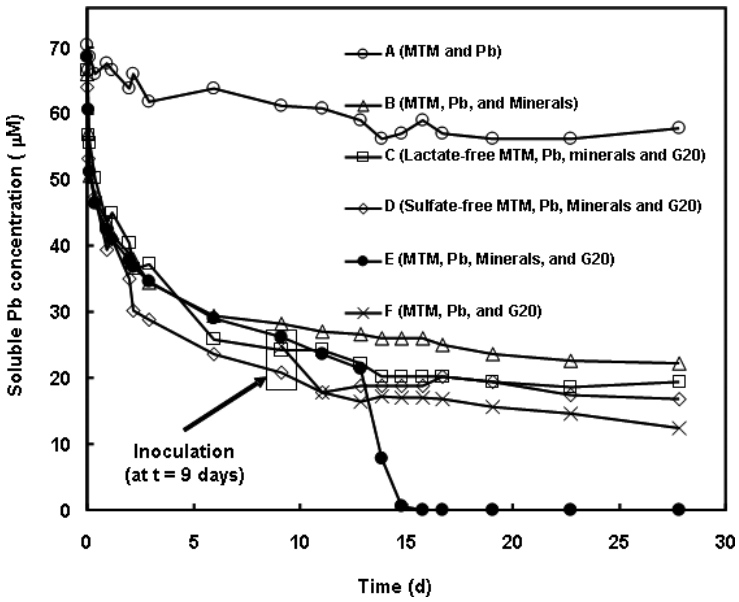

Figure 1. Concentration profiles of soluble Pb during abiotic sorption onto goethite and quartz, and immobilization by *D. desulfuricans* G20. The first 9 d of treatments A, B, C, D, and E consisted abiotic equilibration of Pb. After 9 d, washed *D. desulfuricans* G20 cells were inoculated into three treatments C, D, and E. An additional treatment (F) was also inoculated (t = 9 d) with 26 μm Pb. Other details of these treatments are listed in Table 1.

Immobilization of Pb by *D. desulfuricans* G20

After nine days, when the soluble Pb concentrations roughly stabilized near 26 μM Pb, *D. desulfuricans* G20 cells were inoculated into three treatments (Fig. 1 treatments C, D, and E). Previous studies showed that in MTM (without minerals) *D. desulfuricans* G20 did not grow even at a soluble Pb concentration of 15 μM [27]. To examine the interaction of a mineral phase and soluble Pb concentrations more carefully, two additional treatments were inoculated with *D. desulfuricans* G20 cells at t = 9 days, treatment F (mineral-free control with 26 μM Pb) and treatment G (mineral- and Pb-free control) (Fig. 1; Table 1). More specifically treatment F was started to study the inhibition effects of Pb to *D. desulfuricans* G20 cells in the absence of minerals and treatment G to examine the normal growth pattern of *D. desulfuricans* G20 in-terms of cell protein and soluble sulfide. These treatments, when compared with minerals treatments (C, D, and E), examined the reaction of sulfide produced with minerals.

Table 1. Experimental conditions for abiotic sorption of Pb onto goethite and quartz, and immobilization by *D. desulfuricans* G20.

Treatment (type)	Components	Remarks
A (mineral and *D. desulfuricans* G20-free control)	MTM and Pb	Started with 70 μM Pb at t = 0 d
B (*D. desulfuricans* G20-free control)	MTM, Pb, and minerals	Started with 70 μM Pb at t = 0 d
C (electron donor-free control)	Lactate free-MTM, Pb, minerals, and *D. desulfuricans* G20	Started with 70 μM Pb at t = 0 d *D. desulfuricans* G20 inoculated at t = 9 d
D (electron acceptor-free control)	Sulfate free-MTM, Pb, minerals, and *D. desulfuricans* G20	Started with 70 μM Pb at t = 0 d *D. desulfuricans* G20 inoculated at t = 9 d
E (test)	MTM, Pb, minerals, and *D. desulfuricans* G20	Started with 70 μM Pb at t = 0 d *D. desulfuricans* G20 inoculated at t = 9 d
F (mineral-free control)	MTM, Pb, and *D. desulfuricans* G20	Started with 26 μM Pb at t = 9 d *D. desulfuricans* G20 inoculated at t = 9 d
G (mineral- and Pb-free control)	MTM and *D. desulfuricans* G20	Started with no Pb at t = 9 d *D. desulfuricans* G20 inoculated at t = 9 d
H (Pb-free control)	MTM, minerals, and *D. desulfuricans* G20	Started with no Pb at t = 0 d *D. desulfuricans* G20 inoculated at t = 9 d (protein/sulfide data not shown)
I (mineral-free control with 10 μM Pb)	MTM, Pb, and *D. desulfuricans* G20	Started with 10 μM Pb at t = 9 d *D. desulfuricans* G20 inoculated at t = 9 d (protein/sulfide/Pb data not shown)

In the treatment E (test) containing minerals, *D. desulfuricans* G20 and Pb, the soluble Pb concentration decreased gradually from 26 to 21 μM over four days, but then soluble Pb concentrations decreased rapidly below the detection limit (0.05 μM) over a 3-day period (Fig. 1). However, with all other treatments (A, B, C, D, and F), the soluble Pb concentrations decreased only slightly for the remaining 14 d of experimentation. This slight decrease in soluble Pb concentrations with the mineral (F)-, lactate (C)-, and sulfate (D)-free MTM treatments could have resulted from the following processes: (i) biosorption of Pb to *D. desulfuricans* G20 cells [5], (ii) release of extracellular polymeric substances that can complex Pb [2], (iii) complexation and precipitation of Pb as lead sulfide [27], and (iv) intra-cellular Pb penetration and accumulation [21].

Measurement of *D. desulfuricans* G20 growth during Pb immobilization

As measures of *D. desulfuricans* G20 growth, total cell protein and soluble sulfide were monitored as shown in Fig. 2. It can be seen from Fig. 2a that in treatment G (Pb- and mineral-free controls), *D. desulfuricans* G20 grew after a lag period of two days, but in the presence of Pb and minerals (treatment E), *D. desulfuricans* G20 grew after a lag period of five days. The extent of growth was found to be slightly higher in the treatment E as compared to treatment G. This corroborated with our earlier results where addition of iron compounds (e.g., ferric chloride, goethite, ferrihydrite, or hematite) to MTM (which is an iron-limited medium) enhanced the growth of *D. desulfuricans* G20 [23, 26]. No growth was observed in lactate (C)-and sulfate (D)-free controls (Fig. 2a).

In addition to protein concentrations, the concentration of soluble sulfide increased in *D. desulfuricans* G20 cultures that had measurable growth (Fig. 2b). However, in treatment E (containing Pb, minerals, and *D. desulfuricans* G20), the concentrations of sulfide decreased over time mainly due to the formation of iron sulfides. During the course of these experiments, we observed the color of the solids changed to black, which is characteristic of iron sulfides. In contrast, no decrease in the sulfide concentration was observed in the treatment G (mineral- and Pb-free control) (Fig. 2b).

TEM and EDS analyses of *D. desulfuricans* G20 cells

Figs. 3a and b show TEM images of unstained thin sections of *D. desulfuricans* G20 cells collected from treatment H (Pb-free control). The results showed that most of the precipitates (electron-dense materials) of iron sulfide were present outside the cells, and more than

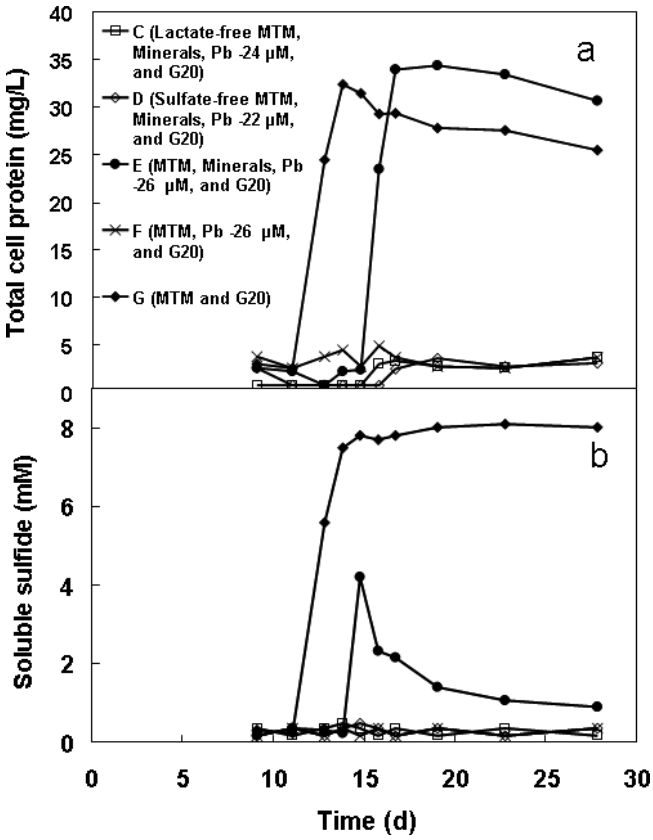

Figure 2. Concentration profiles of total cell protein (a) and soluble sulfide (b) during the growth of *D. desulfuricans* G20. The terminologies of treatments are the same as used in Fig. 1 and listed in Table 1. An additional treatment G (MTM and *D. desulfuricans* G20) was also included to show the normal growth curve of *D. desulfuricans* G20 in absence of Pb and minerals in MTM. Other details are shown in Table 1.

90% of cells had no precipitates associated with their membranes. The analyses of elemental composition of precipitated iron phases by EDS were done by measuring about 20 probe spots. Results showed that Fe and S were the dominant elements in all biogenic precipitates in a 1:1 ratio (Fig. 3c). Iron sulfides likely originated from the reaction of Fe(III) present in goethite with biogenic sulfide ions. Similar iron sulfide precipitates have been shown before in *D. desulfuricans* G20 [12].

Figs. 3d and e show thin sections of *D. desulfuricans* G20 cells recovered from treatment E (containing Pb and minerals). In contrast to treatment H (Pb-free control), cells recovered from treatment E had membrane associated electron dense materials. Interestingly however, again quantitative and qualitative EDS analyses (Fig. 3f) indicated that the electron dense materials were iron sulfides. Multiple EDS spectra of cell-associated and non-cell associated electron dense materials were gathered, but none of the spectra allowed detection

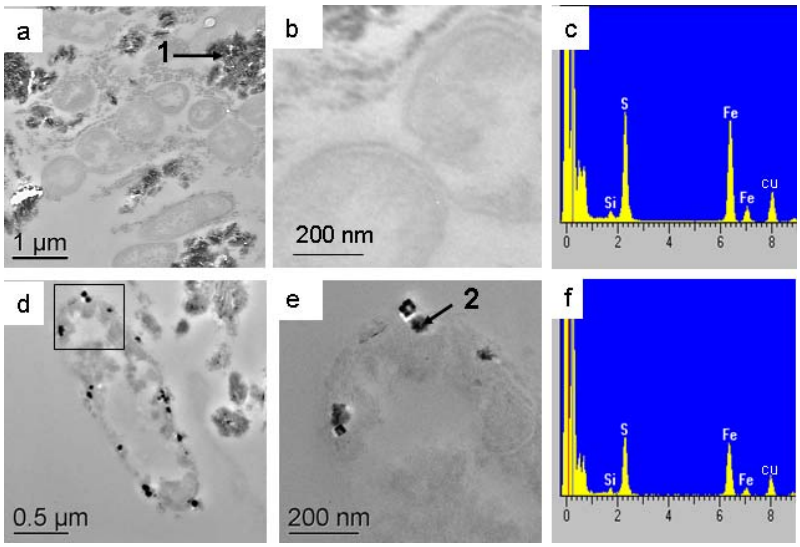

Figure 3. Transmission electron microscopic images of *D. desulfuricans* G20 culture treated with and without 70 µM Pb in metal toxicity medium in the presence of minerals. In Pb-free treatment (Minerals and *D. desulfuricans* G20, treatment H), more than 90% cells had no iron sulfides associated with their membranes (a and b). However, in the presence of Pb (Pb, Minerals, and *D. desulfuricans* G20, treatment E), iron sulfides were found to be associated with the cells (d and e). Apparent precipitates of iron sulfides outside the cells (#1 in a) and associated with the cell surfaces (#2 in e) were confirmed by energy-dispersive X-ray spectroscopy (c and f). Copper background signals in c and f originate from the Cu grid.

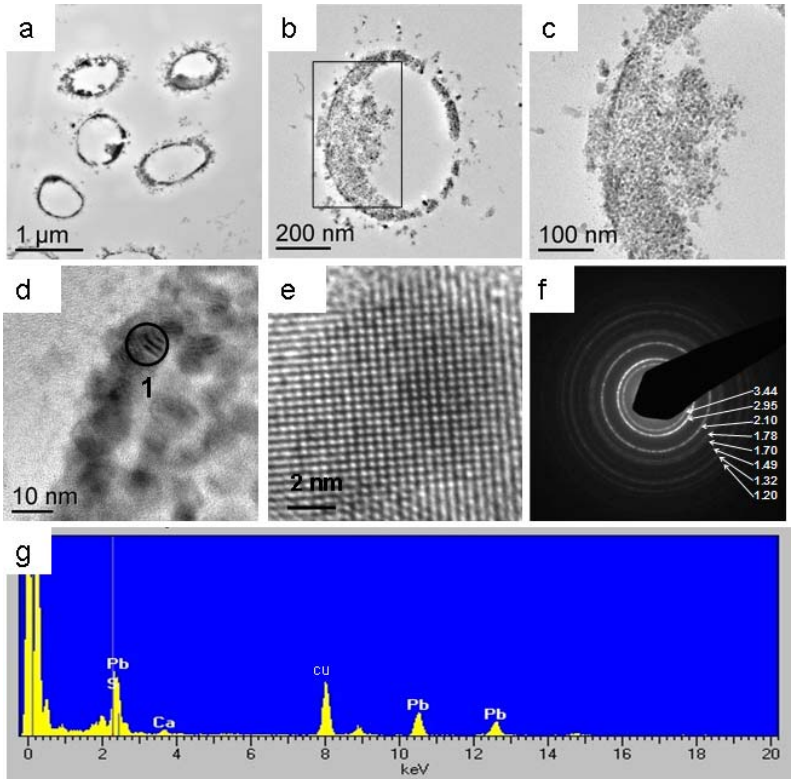

Figure 4. TEM images of *D. desulfuricans* G20 culture treated with 10 µM Pb (treatment I) in metal toxicity medium without minerals. In most of the cells heavy precipitation of biogenic lead sulfide was observed within the periplasm and cytoplasm (a, b, c, and d). HR-TEM image confirms the nanocrystalline character of lead sulfide associated within the bacteria (e). Apparent precipitates of lead sulfide (#1 in d) within the cytoplasmic space were confirmed by selected area electron diffraction pattern (f) and energy-dispersive X-ray spectroscopy (g). The d-spacings values (f) obtained were in a good accordance with the listed galena diffraction data (JCPDS 41-1442). Copper background signal in (g) originates from the Cu grid.

of lead sulfides. The most likely reason for this was that a significantly smaller amount of lead sulfides was present as compared to iron sulfides. Goethite was added to MTM in a considerably higher amount (7503 μmol/l) as compared to Pb (70 μM). Thus, the probability of observing biogenic iron sulfide would be much higher as compared to lead sulfide in the mixture of two.

Figs. 4 a–e show the TEM images of *D. desulfuricans* G20 cells treated with 10 μM Pb in the absence of minerals (treatment I). A majority of observed cells had lead sulfide precipitates both in the periplasm and cytoplasm. SAED and crystallographic analysis of TEM lattice-fringe images showed *d*- spacings of 3.44, 2.95, 2.10, 1.78, 1.70 1.49, 1.32, and 1.20 Å, in excellent agreement with galena as described by the Joint Committee for Powder Diffraction Studies (41-1442) (Fig. 4f). EDS analyses showed the precipitated electron dense materials inside the cells contained Pb and S (Fig. 4g). Thus these combinations of techniques confirmed that Pb precipitated as galena inside the cell.

XRD analyses of precipitates

In treatment B (*D. desulfuricans* G20-free-control, Fig. 5 #B), XRD showed higher intensity peaks at 2θ of 17.8, 21.2, 26.2, 33.2, 36.6, 39.9, 41.2, 50.5, 53.2, 59.0, and 63.2°, which correspond to reflections from goethite. The reflections at 26.6, 45.7, 50.1, 55.5, 59.9, 64.0, and 68.0° correspond to the reflections from quartz. In treatment I (mineral-free control with 10 μM Pb, Fig. 5 #I) the intensities associated with 2θ reflections of 25.9, 30.0, 50.9, 53.4, and 62.6° were ascribed to biogenic lead sulfide (galena) phases. These results on galena were consistent with the results obtained using SAED and EDS as shown in Figs. 4f and g, respectively. In treatment H (Pb-free control, Fig. 5 #H), major peaks belonging to goethite and quartz were observed, but peaks corresponding to biogenic iron sulfides were not detected. We suspect this is due to the formation of amorphous/poorly crystalline nature of iron sulfide phases as reported by Herbert *et al.* [9]. Herbert *et al.* [9] also showed that poorly crystalline iron sulfide phases precipitated in a chemically defined SRB growth medium were composed of both ferric and ferrous iron coordinated with monosulfide, and with lesser amounts of disulfide and polysulfides. The XRD technique is principally for characterizing the crystalline materials and its use for the compounds with amorphous properties is limited [8]. However, major 2θ reflections corresponding to 15.3, 18.3, 21.2, 22.6, 24.9, 31.3, 35.8, and 42.7° in Fig. 5 #H and several other minor reflections corresponding to sulfur (and possibly poly-sulfide) phases were identified. Among these sulfur phases, it

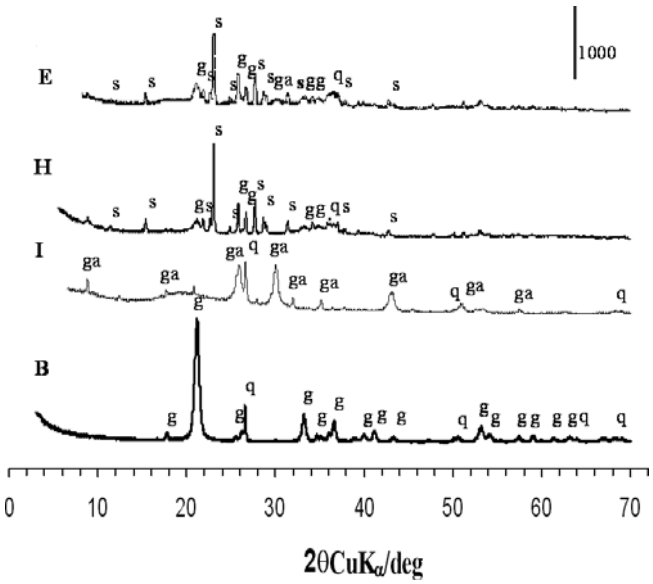

Figure 5. X-ray diffraction patterns of various solids analyzed to determine the formation of galena, and other goethite derived sulfur phases. Treatments B (MTM, Pb, and minerals), E (MTM, Pb, Minerals, and *D. desulfuricans* G20), H (MTM, Minerals, and *D. desulfuricans* G20), and I (MTM, Pb, and *D. desulfuricans* G20) are described in Table 1. Quartz background signal in treatment I originate from the grinding media used in sample preparation for XRD. Vertical bar indicates relative counts. g: goethite; q: quartz; ga: galena; s: sulfur phases.

was very difficult to identify iron-derived sulfur phases (e.g., FeS_2 [pyrite] or FeS_x [pyrrhotite, mackinawite]). Difficulties in identifying iron derived sulfur phases have been encountered earlier by Neal *et al.* [17] while studying the dissolution of hematite (α-Fe_2O_3) by *D. desulfuricans* strains G20 and Essex 6. They used X-ray photoelectron spectroscopy (XPS) to observe a variety of intermediate S species including S^{--}, S_2^{--}, and S_n^{--} similar to that might have formed in the present study. Further studies are needed to identify these sulfur species using various spectroscopic techniques including XPS and Raman spectroscopy.

In treatment E (test, Fig. 5 #E), peaks associated with iron sulfide phases were not detected either, for the same reasons as explained for treatment H (5 #H). However, EDS analyses confirmed the presence of Fe and S in a 1:1 ratio as shown earlier in Fig. 3f. Although in XRD peaks associated with iron sulfide phases were not detected, peaks corresponding to sulfur (11.4 and 23.0°) and lead sulfide phases (30.1°) were distinctly observed suggesting that sulfate-reducing activity resulted in the precipitation of these sulfur and lead sulfide phases. In addition, the goethite peaks (17.7, 33.1, 34.6, and 36.6°) were also detected (Fig. 5 #E).

Biochemical reactions during *D. desulfuricans* G20 growth

At the end of the experiments, the average molar ratio for lactate/sulfate utilization was 1.97 ± 0.07, which is in agreement with the theoretical value of 2 shown by the reaction [30]:

$$2\ CH_3CHOHCOO^- + SO_4^{--} + H^+ \rightarrow 2\ CH_3COO^- + 2\ CO_2 + 2\ H_2O + HS^- \quad (1)$$

Similarly, the average molar ratio for lactate consumption to acetate production was 0.98 ± 0.03, which is in agreement with the theoretical value of 1 for reaction 1. Therefore, these results suggest that sulfate reduction proceeded according to reaction 1. The detection of iron sulfide and possibly elemental sulfur suggest that goethite was abiotically reduced by biogenic sulfide according to the reaction (2) with subsequent precipitation of iron sulfides (reaction 3):

$$16\ FeOOH_{(s)} + 8\ HS^- + 40\ H^+ \rightarrow 16\ Fe^{++} + S_{8(s)} + 32\ H_2O \quad (2)$$

$$Fe^{++} + HS^- \rightarrow FeS_{(s)} + H^+ \quad (3)$$

D. desulfuricans G20 can also enzymatically reduce Fe(III) using lactate as an electron donor (reaction 4); however, such activity appeared to be limited in this study, as indicated by the molar ratio of lactate/sulfate very close to 2, suggesting that reaction (1) likely contributed to lactate consumption.

$$2\ CH_3CHOHCOO^- + 8\ FeOOH_{(s)} + 16\ H^+ \rightarrow 2\ CH_3COO^- + 2\ CO_2 + 14\ H_2O + 8\ Fe^{++} \quad (4)$$

Toxicity of Pb to *D. desulfuricans* G20 and the effect of minerals

Previous Pb toxicity studies on *D. desulfuricans* G20 [22, 27] showed that growth of *D. desulfuricans* G20 began only when the soluble Pb concentration decreased to near the ICP-MS detection limit (0.05 μM). In contrast to these previous results, in the presence of goethite and quartz, even at 26 μM soluble Pb, *D. desulfuricans* G20 grew well after a lag time of 5 d (ANOVA, $p = 0.0001$) (treatment E, Fig. 2). This was surprising since previous findings showed that in the absence of minerals, no growth was observed at Pb concentrations ≥15 μM even in 30 d of incubation [22, 27]. In this study in parallel mineral-free controls with 26 μM soluble Pb (treatment F, Fig. 2), no growth of *D. desulfuricans* G20 was observed even after 20 days. These results clearly show that at the same soluble concentration of Pb (26 μM), the presence of goethite and quartz in MTM significantly decreased the apparent toxicity of Pb to *D. desulfuricans* G20.

Mechanisms of Pb resistance in *D. desulfuricans* G20 and the effect of minerals

The toxicity of heavy metals to microbes depends upon its bioavailability [3]. A metal is considered to be bioavailable when it can be taken up by organisms and is subsequently accessible to the physiological processes upon which it exerts an effect. Goethite is known to strongly adsorb heavy metals, consequently reducing toxicant availability to the microorganisms. In addition, adhesion of microbes to mineral surfaces is well known to play an important role in protection from biocidal compounds through numerous mechanisms including diffusion limitations and changes in physiology of attached microorganisms [3]. SEM results showed that *D. desulfuricans* G20 cells were surrounded by goethite crystals which likely acted as a sorption and diffusion barrier significantly decreasing the local bioavailability of Pb to *D. desulfuricans* G20 (Fig. 6). Fig. 6a shows a single *D. desulfuricans* G20 cell surrounded by goethite crystals. Even under shaking conditions, some mineral-associated *D. desulfuricans* G20 cells were likely protected enough to grow and reduce sulfate to sulfide which reacted with iron and/or Pb to form black metal sulfide precipitates. Fig. 6b, taken only four days after inoculation, shows initiation of localized growth as indicated by the black metal-sulfide precipitates of iron and/or Pb. The formation of a lead sulfide precipitates would have further decreased local Pb bioavailability allowing the colony to be less inhibited by Pb. It has been shown using Live/Dead staining that Pb does not rupture *D. desulfuricans* G20 cell membranes [22, 27], so that even at Pb concentrations that utterly inhibit growth *D. desulfuricans* G20 cells may not die. Ultimately, as shown in Fig. 1, with sulfate-reducing activity, Pb concentrations decreased to levels that allow more widespread *D. desulfuricans* G20 growth and eventual precipitation of all measureable soluble Pb.

Results showed that the presence of goethite and quartz decreased Pb (26 μM $PbCl_2$) toxicity to *D. desulfuricans* G20 significantly. Using HR-TEM and XRD techniques we showed that (i) in the absence of goethite and quartz, *D. desulfuricans* G20 likely detoxified Pb using both uptake (formation of PbS inside the cells) and sulfide precipitation mechanisms; however, in the presence of goethite and quartz, sulfide precipitation mechanism was dominant (since no Pb was observed inside the cells under these conditions) and (ii) *D. desulfuricans* G20 treated with goethite, quartz, and $PbCl_2$ showed the presence of a dense deposit of iron sulfide precipitates both in the periplasm and cytoplasm indicating that *D. desulfuricans* G20 took up Fe inside the cell. In SRB, it is believed that the predominant mecha-

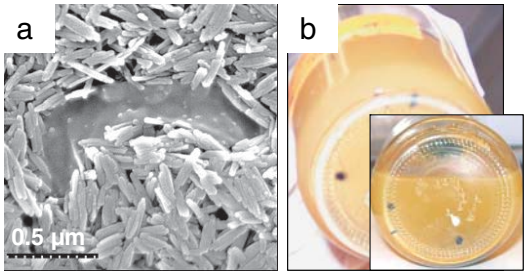

Figure 6. Scanning electron microscopic images of (a) *D. desulfuricans* G20 cells attached to goethite minerals immediately after inoculation (b) Black colonies show the growth of *D. desulfuricans* G20 in serum bottle after 4 d of inoculation.

nism of metal detoxification is indirect metal precipitation by biogenic H_2S [15]. In order to prevent the formation of metal precipitates, MTM used in our study had no specifically added carbonate or phosphate [22]. Such a modification in medium component could also alter the physiology of *D. desulfuricans* G20, stimulating uptake systems that might allow access of toxic metals (e.g., Pb) into the cytoplasm. Further fundamental research is needed in both suspended and attached microbial systems to make significant improvements in understanding of interactions of microorganisms to metals and minerals.

Concluding remarks

Microbial Pb inhibition and detoxification in the presence of soil minerals are poorly understood, especially in SRB, even though these organisms play an important role in metal sequestration in subsurface soils and groundwater. Our laboratory experiments evaluated the effects of Pb inhibition and detoxification to *D. desulfuricans* G20 in the presence of goethite and quartz. Addition of minerals to MTM resulted in an apparent decrease in Pb toxicity to *D. desulfuricans* G20 even at the same soluble Pb concentration which utterly inhibited growth in the absence of goethite and quartz. TEM analyses showed that detection of lead or iron sulfides inside the *D. desulfuricans* G20 cells was dependent on the presence of goethite and quartz. While the results obtained using MTM, a pure culture of *D. desulfuricans* G20, goethite, and quartz are not directly applicable to natural environments where several chemical complexants and other microorganisms are present, the results presented here have fundamental relevance to (i) SRB found in natural systems that contain Pb and soil minerals, (ii) elucidating mechanisms of metal resistance in natural systems, and (iii) to efforts to use SRB for *in situ* immobilization of Pb.

Acknowledgements

The authors gratefully acknowledge the financial support provided by the Natural and Accelerated Bioremediation Research program (now known as Environmental Remediation Science Program, Office of Biological and Environmental Research, U.S. Department of Energy (Grants #DE-FG03-98ER62630/A001, #DE-FG03-01ER63270, and #DE-FG02-07-ER-64366) and National Science Foundation Grant No. 0628258. In addition, Rajesh Sani acknowledges funding through the South Dakota Governors 2010 seed grant program. The HR-TEM imaging and analyses were performed at the W. R. Wiley Environmental Molecular Sciences Laboratory (EMSL), a national scientific user facility operated by Battelle for the U.S. DOE, located at the Pacific Northwest National Laboratory in Richland, WA. We also thank the anonymous reviewers whose critiques were instrumental in improving the quality of our manuscript.

References

[1] Bagwell, C.E., Liu, X., Wu, L. and Zhou, J., 2006. Effects of legacy nuclear waste on the compositional diversity and distributions of sulfate-reducing bacteria in a terrestrial subsurface aquifer. FEMS Microbiol. Ecol., **55**, 424–431.

[2] Beech, I.B. and Cheung, C.W.S., 1995. Interactions of exopolymers produced by sulfate-reducing bacteria with metal ions. Int. Biodet. Biodeg., **35**, 59–72.

[3] Brown, G.E. Jr., Foster, A.L. and Ostergren, J.D., 1999. Mineral surfaces and bioavailability of heavy metals: a molecular-scale perspective. Proc. Natl. Acad. Sci., USA **96**, 3388–3395.

[4] Cabrera, G., Pérez, R., Gómez, J.M., Abalos, A. and Cantero, D., 2006. Toxic effects of dissolved heavy metals on *Desulfovibrio vulgaris* and *Desulfovibrio* sp. strains. J. Hazard. Mater., **135**, 40–46.

[5] EI-Bayoumy M.A., Bewtra, J.K., Ali, H.I. and Biswas, N., 1997. Biosorption of lead by biomass of sulfate reducing bacteria. Can. J. Civil. Engineer., **24**, 840–843.

[6] Eick, M.J., Peak, J.D., Brady, P.V. and Pesek, J.D., 1999. Kinetics of lead adsorption/desorption on goethite: residence time effect. Soil. Sci., **164**, 28–39.

[7] Fredrickson, J.K., Zachara, J.M., Kennedy, D.W., Dong, H., Onstott, T.C., Hinman, N.W. and Li, S., 1998. Biogenic iron mineralization accompanying the dissimilatory reduction of hydrous ferric oxide by a groundwater bacterium. Geochim. Cosmochim. Acta., **62**, 3239–3257.

[8] Guinier, A., 1994. X-ray diffraction in crystals, imperfect crystals, and amorphous bodies: In crystals, imperfect crystals, and amorphous Bodies Published by Courier Dover Publications, ISBN 0486680118.

[9] Herbert, R.B., Benner, S.G., Pratt, A.R. and Blowes, D.W., 1998. Surface chemistry and morphology of poorly crys-

talline iron sulfides precipitated in media containing sulfate-reducing bacteria. Chem. Geol., **144**, 87–97.

[10] Karnachuk, O.V., Sasaki, K., Gerasimchuk, A.L., Sukhanova, O., Ivasenko, D.A., Kaksonen, A.H., Puhakka, J.A. and Tuovinen, O.H., 2008. Precipitation of Cu-sulfides by copper-tolerant *Desulfovibrio* isolates. Geomicrobiol. J., **25**, 219–227.

[11] Legodi, M.A. and de Waal, D., 2007. The preparation of magnetite, goethite, hematite and maghemite of pigment quality from mill scale iron waste. Dyes and Pigments **74**, 161–168.

[12] Li, Y.L., Vali, H., Yang, J., Phelps, T.J. and Zhang, C.L., 2006. Reduction of iron oxides enhanced by a sulfate-reducing bacteria and biogenic H_2S. Geomicrobiol. J., **23**, 103–117.

[13] Lloyd, J.R. and Lovley, D.R., 2001. Microbial detoxification of metals and radionuclides. Curr. Opinion. Biotechnol., **12**, 248–253.

[14] McCullough, J., Hazen, T.C., Benson, S.M., Metting, F.B. and Palmisano, A.C., 2004. Bioremediation of metals and radionuclides: what it is and how it works. Lawrence Berkeley National Laboratory report 42595, 2nd ed. Lawrence Berkeley National Laboratory, Berkeley, Calif.

[15] Muyzer, G. and Stams, A.J., 2008. The ecology and biotechnology of sulphate-reducing bacteria. Nat. Rev. Microbiol., **6**, 441–454.

[16] Naz, N., Young, H.K., Ahmed, N. and Gadd, G.M., 2005. Cadmium accumulation and DNA homology with metal resistance genes in sulfate-reducing bacteria. Appl. Environ. Microbiol., **71**, 4610–4618.

[17] Neal, A.L., Techkarnjanaruk, S., Dohnalkova, A., McCready, D., Peyton, B.M. and Geesey, G.G., 2001. Iron sulfides and sulfur species produced at hematite surfaces in the presence of sulfate-reducing bacteria. Geochim. Cosmochim. Acta., **65**, 223–235.

[18] O'Day, P.A., Vlassopoulos, D., Root, R. and Rivera, N., 2004. The influence of sulfur and iron on dissolved arsenic concentrations in the shallow subsurface under changing redox conditions. Proc. Natl. Acad. Sci., USA, **101**, 13703–13708.

[19] Poulson, S.R., Colberg, P.J.S. and Drever, J.I., 1997. Toxicity of heavy metals (Ni, Zn) to *Desulfovibrio desulfuricans*. Geomicrobiol. J., **14**, 41–49.

[20] Riley, R.G., Zachara, J.M. and Wobber, F.J., 1992. Chemical contaminants on DOE lands and selection of contaminant mixtures for subsurface research, DOE/ER-0547T, U.S. Department of Energy, Washington, D.C.

[21] Roane, T.M., 1999. Lead resistance in two bacterial isolates from heavy metal-contaminated soils. Microb. Ecol., **37**, 218–224.

[22] Sani, R.K., Geesey, G.G. and Peyton, B.M., 2001. Assessment of lead toxicity to *Desulfovibrio desulfuricans* G20: influence of components of lactate C medium. Adv. Environ. Res., **5**, 269–276.

[23] Sani, R.K., Peyton, B.M., Amonette, J.E. and Geesey, G.G., 2004. Reduction of uranium(VI) under sulfate reducing conditions in the presence of Fe(III)-(hydr)oxides. Geochim. Cosmochim. Acta, **68**, 2639–2648.

[24] Sani, R.K., Peyton, B.M. and Brown. L.T., 2001. Copper-induced inhibition in growth of *Desulfovibrio desulfuricans* G20: assessment of its toxicity and correlation with zinc and lead. Appl. Environ. Microbiol., **67**, 4765–4772.

[25] Sani, R.K., Peyton, B.M. and Dohnalkova, A., 2006. Toxic effects of uranium on *Desulfovibrio desulfuricans* G20. Environ. Toxicol. Chem., **25**, 1231–1238.

[26] Sani, R.K., Peyton, B.M., Dohnalkova, A. and Amonette, J.E., 2005. Reoxidation of reduced uranium with iron(III) (hydr)oxides under sulfate-reducing conditions. Environ. Sci. Technol., **39**, 2059–2066.

[27] Sani, R.K., Peyton, B.M. and Jandhyala, M., 2003. Toxicity of lead in aqueous medium to *Desulfovibrio desulfuricans* G20. Environ. Toxicol. Chem., **22**, 252–260.

[28] Schwertmann, U. and Cornell, R.M., 1991. Iron oxides in the laboratory, preparation and characterization. VSH Publishers, New York, USA.

[29] Shotyk, W. and Le Roux, G., 2005. Biogeochemistry and cycling of lead. Met. Ions. Biol. Syst., **43**, 239–275.

[30] Thauer, R.K., Jungerman, K. and Decker, K., 1977. Energy conservation in chemotrophic anaerobic bacteria. Bacteriol. Rev., **41**, 100–180.

[31] Utgikar, V.P., Tabak, H.H., Haines, J.R. and Govind, R., 2003. Quantification of toxic and inhibitory impact of copper and zinc on mixed cultures of sulfate-reducing bacteria. Biotechnol. Bioeng., **82**, 306–312.

[32] Viamajala, S., Peyton, B.M., Sani, R.K., Apel, W.A. and Petersen, J.N., 2004. Toxic effects of chromium(VI) on anaerobic and aerobic growth of *Shewanella oneidensis* MR-1. Biotechnol. Prog., **20**, 87–95.

[33] White, C., Sharman, A.K. and Gadd, G.M., 1998. An integrated microbial process for the bioremediation of soil contaminated with toxic metals. Nat. Biotechnol., **16**, 572–575.

